AGU PUBLICATIONS

JGR

Journal of Geophysical Research: Biogeosciences

RESEARCH ARTICLE
10.1002/2013JG002600

Key Points:
- Humic DOM is susceptible to microbial degradation along with peptide-like DOM
- Labile DOM can be distinguished from recalcitrant DOM in van Krevelen space
- EEMs and FTICR-MS chemically characterize bioreactive and recalcitrant DOM

Correspondence to:
R. L. Sleighter,
rsleight@odu.edu

Citation:
Sleighter, R. L., R. M. Cory, L. A. Kaplan, H. A. N. Abdulla, and P. G. Hatcher (2014), A coupled geochemical and biogeochemical approach to characterize the bioreactivity of dissolved organic matter from a headwater stream, *J. Geophys. Res. Biogeosci.*, *119*, 1520–1537, doi:10.1002/2013JG002600.

Received 20 DEC 2013
Accepted 13 JUL 2014
Accepted article online 17 JUL 2014
Published online 8 AUG 2014

A coupled geochemical and biogeochemical approach to characterize the bioreactivity of dissolved organic matter from a headwater stream

Rachel L. Sleighter[1], Rose M. Cory[2], Louis A. Kaplan[3], Hussain A. N. Abdulla[1], and Patrick G. Hatcher[1]

[1]Department of Chemistry and Biochemistry, Old Dominion University, Norfolk, Virginia, USA, [2]Earth and Environmental Sciences, University of Michigan, Ann Arbor, Michigan, USA, [3]Stroud Water Research Center, Avondale, Pennsylvania, USA

Abstract The bioreactivity or susceptibility of dissolved organic matter (DOM) to microbial degradation in streams and rivers is of critical importance to global change studies, but a comprehensive understanding of DOM bioreactivity has been elusive due, in part, to the stunningly diverse assemblages of organic molecules within DOM. We approach this problem by employing a range of techniques to characterize DOM as it flows through biofilm reactors: dissolved organic carbon (DOC) concentrations, excitation emission matrix spectroscopy (EEMs), and ultrahigh resolution mass spectrometry. The EEMs and mass spectral data were analyzed using a combination of multivariate statistical approaches. We found that 45% of stream water DOC was biodegraded by microorganisms, including 31–45% of the humic DOC. This bioreactive DOM separated into two different groups: (1) H/C centered at 1.5 with O/C 0.1–0.5 or (2) low H/C of 0.5–1.0 spanning O/C 0.2–0.7 that were positively correlated (Spearman ranking) with chromophoric and fluorescent DOM (CDOM and FDOM, respectively). DOM that was more recalcitrant and resistant to microbial degradation aligned tightly in the center of the van Krevelen space (H/C 1.0–1.5, O/C 0.25–0.6) and negatively correlated (Spearman ranking) with CDOM and FDOM. These findings were supported further by principal component analysis and 2-D correlation analysis of the relative magnitudes of the mass spectral peaks assigned to molecular formulas. This study demonstrates that our approach of processing stream water through bioreactors followed by EEMs and FTICR-MS analyses, in combination with multivariate statistical analysis, allows for precise, robust characterization of compound bioreactivity and associated molecular level composition.

1. Introduction

Dissolved organic matter (DOM) transported by freshwaters contributes approximately 1.2 Pg of CO_2 to the atmosphere annually, with the potential for feedbacks on global climate change as bioreactive DOM is metabolized to CO_2 primarily by heterotrophic microorganisms in streams and rivers [*Richey et al*., 2002; *Sabine et al*., 2004; *Cole et al*., 2007; *Battin et al*., 2009; *Tranvik et al*., 2009]. This underscores the substantial amount of metabolic energy that rivers transport to downstream ecosystems [*Kaplan and Newbold*, 1993; *Mayer et al*., 1998; *Cole and Caraco*, 2001; *Grace and Malhi*, 2002; *Battin et al*., 2008; *Aufdenkampe et al*., 2011]. However, while quantifying transformations and fluxes of DOM in inland waters is important to estimates of net changes in the global C cycle, uptake rates for trace fractions of the molecularly recognizable compounds such as carbohydrates and amino acids [*Kirchman*, 2003; *Benner*, 2003] only account for <20% of the organic carbon required to support microbial respiration in stream ecosystems [*Volk et al*., 1997; *Kaplan and Newbold*, 2003; *Kaplan et al*., 2008].

Recently, we produced evidence strongly supporting the idea that molecularly uncharacterized humic substances contribute to the labile and semilabile DOM pool in stream water by analyzing the chromophoric and fluorescent fractions of DOM (CDOM and FDOM, respectively), which are proxies for DOM source and relative bioreactivity [*Cory and Kaplan*, 2012]. Analysis of CDOM and FDOM provides insights into the different types of carbon within the DOM pool hypothesized to differ in bioreactivity to microbial heterotrophs: carbon associated with humic substances derived from either terrigenous or microbial sources and carbon associated with free or combined fluorescent amino acids, specifically tryptophan, tyrosine, and phenylalanine. As expected, amino acid-like FDOM was found to be more susceptible to biodegradation than the humic-like FDOM, but amino acids account for a small fraction of C in the DOM pool (about 2%), while the majority (>50%)

of the aquatic DOM pool is classified as humic C. Mass balance arguments demonstrate that the observed 4–20% loss of humic FDOM [*Cory and Kaplan*, 2012] must account for the majority of the DOM pool labile to microorganisms. Further support for the role of humic DOM in the biodegradable fractions of DOM has been provided by a positive correlation between humic FDOM and DOM uptake by microorganisms [*Mann et al*., 2012], as well as direct measurements of lignin and polyphenol degradation in river water incubations [*Ward et al*., 2013], selective bacterial degradation and demethylation of lignin residues in stream water DOM in laboratory-scale bioreactors [*Frazier et al*., 2005], and degradation of stream water humic substances measured with XAD-8 resin and laboratory-scale bioreactors [*Volk et al*., 1997].

Thus, while fractions of CDOM and FDOM most bioreactive to microbial degradation are consistent with the conceptual model of the very labile fraction of DOM as low molecular weight, N-rich amino acids [*Hopkinson et al*., 1998; *Michaelson et al*., 1998; *Cleveland et al*., 2004; *Wickland et al*., 2007; *Fellman et al*., 2008, 2009a, 2009b; *Balcarczyk et al*., 2009; *Hood et al*., 2009; *Guillemette and del Giorgio*, 2011; *Cory and Kaplan*, 2012; *Mann et al*., 2012], clearly humic C contributes to the biodegradable DOM pool as well [*Wetzel*, 2003]. However, CDOM and FDOM are general categories for compound classes based on correlations to aromatic carbon content [*McKnight et al*., 2001; *Cory and McKnight*, 2005], terrestrial or microbial precursor material [*McKnight et al*., 2001; *Cory and McKnight*, 2005], free or combined amino acids [*Yamashita and Tanoue*, 2003], and C/N ratios and isotopic signatures of organic nitrogen within DOM [*Cory et al*., 2007]. We currently know too little about the molecular features of the biodegradable humic DOM and need to find a way to organize and quantify the detailed molecular level data that provide insights into this important C pool.

We developed a novel approach to organize and quantify the detailed molecular level data on the biodegradable humic fraction of DOM using innovative laboratory-based plug-flow biofilm reactors [*Kaplan et al*., 2008] to separate stream water DOM into labile, semilabile, and recalcitrant bioreactivity pools, adapted from the concepts of organic matter bioreactivity that have been developed for marine DOM [*Carlson*, 2002]. While these three bioreactivity classes are empirically derived and simplify what likely is a continuum of bioreactivities [*Cummins et al*., 1972; *Vähätalo et al*., 2010; *Koehler et al*., 2012], we examine the composition of DOM in each pool using optical methods (e.g., CDOM and FDOM) in tandem with electrospray ionization Fourier transform ion cyclotron resonance mass spectrometry (ESI-FTICR-MS). FTICR-MS provides the most resolved view of DOM composition by generating a mass spectrum containing thousands of peaks [*Marshall et al*., 1998; *Stenson et al*., 2003; *Kim et al*., 2006; *Sleighter and Hatcher*, 2007; *Reemtsma*, 2009], each likely representing numerous compounds having the same molecular formulas but different structures [*Sleighter and Hatcher*, 2008, 2011]. Peaks are mainly in the region of 200–800 m/z and singly charged so that m/z represents molecular ions [*Stenson et al*., 2002]. While this approach will yield bulk compositional information for DOM, its most powerful advantage is that each of the thousands of resolved peaks can be assigned unique molecular formulas to differentiate the elemental composition of DOM compounds. Thus, in this study, laboratory-based plug-flow bioreactors separated DOM into empirically derived classes of bioreactive compounds, and FTICR-MS, in combination with the analysis of CDOM and FDOM, was utilized to identify the composition of the formulas within these classes.

The bioreactors utilize colonized stream microorganisms to biodegrade stream water DOM as it passes through reactors varying in size and thus residence time. Gradients of heterotrophic microbial densities, community composition, and physiological capabilities form from the inflow to the outflow within the bioreactors, along with gradients of DOM concentration and quality. We exploited these gradients to obtain bioreactor effluents of different bioreactivity as the most biologically labile DOM molecules are rapidly metabolized (over short bioreactor volumes), semilabile DOM molecules are metabolized after longer exposures, and more recalcitrant DOM molecules exit the bioreactors without being metabolized [*Kaplan and Newbold*, 1995]. Empty bed contact times (EBCTs) (i.e., volume divided by the flow rate), or residence times (i.e., the length of time that DOM is available for biological uptake), is a surrogate for DOM bioreactivity, with the bioreactor effluents becoming increasingly devoid of bioreactive DOM as the EBCT increases. By establishing a series of bioreactors with increasing EBCTs, we could collect effluents that fall along a chemical gradient of declining bioreactivity and analyze their concentration and composition.

The three main goals of this study were to (1) elucidate the biological reactivity of molecules present in stream water, (2) understand how DOM bioreactivity can be related to its chemical composition, and (3) relate DOM optical properties to molecular composition and reactivity. Linear regressions and multivariate statistical analyses were conducted to identify the molecular features of the biodegradable humic DOM pool

along the chemical gradient of declining bioreactivity. We demonstrate that our approach can serve to connect the geochemical measures of DOM composition with the biogeochemical measures of function and place these within the context of energy flow in stream ecosystems.

2. Methods

2.1. Sample Collection and Bioreactor Operation

Stream water (5 L) from White Clay Creek was collected in November 2011 from a 20 cm deep section of the stream in a precombusted (480 °C, 6 h) borosilicate glass bottle. The water was brought into the laboratory, filtered immediately, and loaded onto plug-flow bioreactors to separate DOM into different bioreactivity classes [*Kaplan et al*., 2008; *Cory and Kaplan*, 2012]. White Clay Creek, previously described in detail [*Newbold et al*., 1997], is a third-order stream with intact riparian woodlands in the southeastern Pennsylvania Piedmont (39°53′N, 75°47′W). The stream water was filtered through a three stage Balston glass fiber cartridge system of nominal 75, 25, and 0.3 μm filters in series that remove larger particles but allow approximately 95% of the bacteria suspended in the stream water to pass into the filtrate.

Filtrate was pumped into the bottom of bioreactors under pressure at 4 mL min^{-1} [*Kaplan and Newbold*, 1995]. The bioreactors are chromatography columns filled with sintered glass beads that are kept in the dark in a temperature controlled room (20 °C) and colonized by microorganisms contained within and nourished from a continuous input of stream water [*Kaplan and Newbold*, 1995]. We established nine bioreactors with EBCTs that increased in a geometric series (0.5, 1.5, 3, 6, 9, 37, 73.8, 150, and 271.5 min). The slow perfusion of water through the bioreactors reduces the effective horizontal distance (or vertical depth in the water column) that molecules need to pass through to contact biofilms, compared to a stream water column. Prior studies comparing the behavior of a ^{13}C DOM tracer in the bioreactors and in whole stream injections were used to develop an appropriate scaling to facilitate the transfer of information obtained in the laboratory to the environment and determine that reactions that occur in the bioreactors over time scales of minutes and moving through spatial scales of centimeters occur in the stream at equivalent dimensions of time scales ranging from hours to days and spatial scales ranging from hundreds of meters to kilometers [*Kaplan et al*., 2008].

Filtrate used to feed the bioreactors and bioreactor effluents were collected in clear precombusted borosilicate glass vessels with persulfate-cleaned silicon-backed Teflon® septa. Three bioreactor bed volumes were passed to waste prior to sample collection. Dissolved organic carbon (DOC) concentrations were measured by UV-catalyzed persulfate oxidation with conductimetric detection (Sievers 900 analyzer, Boulder, CO, USA) within 1 day of sample collection. A five-point external calibration of the Sievers 900 instrument was performed with potassium hydrogen phthalate standards. Following the procedure from the manufacturer, seven replicate blank measurements were used to determine the limit of detection (3 times standard deviation) and the limit of quantification (10 times standard deviation), and these values were 2.4 μg C/L and 8.9 μg/L, respectively. Instrument precision, expressed as the average coefficient of variation for duplicate analyses of the inflow and outflow samples, was 0.55% ± 0.45% (n = 10). Biodegradable DOC (BDOC) concentrations were calculated as the difference between the DOC concentration in the influent and effluent waters [*Kaplan and Newbold*, 1995]. The bioreactor data of declining DOC concentration with increasing EBCT were fit to a three-pool G model consisting of the sum of exponential decay terms for three bioreactivity pools: labile (C_1) and semilabile (C_2) constituents plus a nondegradable (recalcitrant) pool (C_3) [*Westrich and Berner*, 1984].

Subsamples of the influent stream water and effluent waters from the first eight bioreactors (excluding EBCT 271.5 min) were immediately placed on ice and shipped cold via overnight courier for subsequent analyses of DOM quality.

2.2. Excitation Emission Matrix Fluorescence Spectroscopy

Optical properties of DOM in water samples were analyzed by UV–vis and fluorescence spectroscopy as previously described in detail [*Cory and Kaplan*, 2012]. The spectral slope ratio (S_R) was calculated from the absorbance spectrum of each sample according to *Helms et al*. [2008]. Naperian absorption coefficients, a_λ, were calculated at specific wavelengths as follows:

$$a_\lambda = \frac{A_\lambda}{l} 2.303$$

where *A* is the absorbance reading and *l* is the path length in meters. The fluorescence index (FI) was calculated as the ratio of emission intensity at 470 nm to 520 nm obtained at an excitation wavelength of 370 nm [*McKnight et al*., 2001; *Cory et al*., 2010a].

Parallel factor analysis (PARAFAC) was utilized to separate the data set of EEMs of White Clay Creek water passing through the bioreactors, as previously described [*Cory and Kaplan*, 2012]. PARAFAC separates a data set of EEMs into mathematically and chemically independent components (each representing a single fluorophore or a group of strongly covarying fluorophores) multiplied by their excitation and emission spectra (representing either pure or combined spectra). All five components in White Clay Creek water previously validated by PARAFAC analysis [*Cory and Kaplan*, 2012] were nearly identical to components commonly identified in surface waters [*Cory and McKnight*, 2005; *Stedmon and Markager*, 2005]. Components C2 and C3 give rise to the ubiquitously identified humic-like peaks A and C, respectively [*Coble*, 1996], and are relatively enriched in the hydrophobic humic substances fraction of DOM relative to unfractionated DOM in filtered water [*Cory et al*., 2007], as distinguished by XAD-8 chromatographic separation of humic substances [*Aiken et al*., 1992]. Further, humic-like fluorophores represented by C2 and C3 have been associated with terrestrially derived material such as lignin breakdown products [*Hernes et al*., 2009], aromatic carbon content [*Cory and McKnight*, 2005; *Cory et al*., 2007], and DOM having the optical properties of degraded lignin [*Del Vecchio and Blough*, 2004]. The excitation and emission maxima of C1, also considered a humic-like fraction of DOM, correspond to recent autochthonous production [*Murphy et al*., 2008]. Protein-like components C4 and C5 have excitation and emission maxima in the amino acid region, with C4 overlapping with an amino acid-like component most similar to tryptophan while C5 closely resembles tyrosine [*Cory and McKnight*, 2005; *Stedmon and Markager*, 2005].

We employed the standard approach to quantifying and comparing changes in DOM components based on comparison of the F_{max} value of each component in each sample, which provides an estimate of the relative concentration of each component. Estimates for the precision of the F_{max} values of each component were obtained from the triplicate analyses of each sample [*Cory and Kaplan*, 2012].

2.3. Electrospray Ionization Fourier Transform Ion Cyclotron Resonance Mass Spectrometry

Nine samples described above (stream water and eight bioreactor samples) were prepared for mass spectral analysis using PPL solid phase extraction cartridges (Agilent, Bond Elut PPL, 100 mg resin, 3 mL volume), according to the procedure recommended by *Dittmar et al*. [2008]. Approximately 500 mL of each sample were acidified to a pH of 2 (with 12 M trace metal grade HCl) and extracted through the PPL cartridges conditioned with MeOH and H_2O (all LC-MS grade), ensuring that the flow rate was always less than 25 mL/min. After extraction, the cartridges were rinsed with 2 column volumes of acidified H_2O and dried under N_2 gas. DOM was eluted from the cartridges by gravity with 8 mL of MeOH.

The PPL extracted samples in MeOH were diluted by 2 with H_2O containing NH_4OH immediately prior to mass spectral analysis, giving a final sample composition of 1:1 (v/v) MeOH: H_2O with 0.05% NH_4OH. The samples were continuously infused into an Apollo II ESI ion source of a Bruker Daltonics 12 Tesla Apex Qe FTICR-MS, introduced by a syringe pump operating at 120 $\mu L\,hr^{-1}$. ESI voltages were optimized for each analysis using a spray shield voltage of 3.3–3.5 kV and a capillary voltage of 4.0–4.2 kV, yielding consistent and stable ESI spray shield and capillary currents of 180–210 nA and 20–30 nA, respectively. Ions were accumulated for 0.4 s in a hexapole before being transferred to the ICR cell, where 300 transients, collected with a 4 MWord time domain, were coadded, giving about a 25 min total run time. The summed FID signal was zero-filled once and Sine-Bell apodized prior to fast Fourier transformation and magnitude calculation using the Bruker Daltonics Data Analysis software.

Prior to data analysis, all samples were externally calibrated with a polyethylene glycol standard and internally calibrated with fatty acids, dicarboxylic acids, and other naturally present compounds that are part of various CH_2 homologous series [*Sleighter et al*., 2008]. All *m/z* lists, created using a signal to noise (S/N) threshold of 3, were exported for further analysis. Of the nine samples analyzed, three were analyzed in duplicate to assess the reproducibility of the FTICR-MS acquisitions. Mass lists (constructed using S/N ≥ 3) were corrected using S/N ≥ 2.5, according to *Sleighter et al*. [2012], and common peak percentages for the three samples were 84% on average (range of 82-86%). Peak magnitudes were also found to be reproducible, as the average percent relative standard deviation (RSD) for all three duplicate analyses was ≤8%, and 70–71% of the peaks had peak

magnitude ratios (as described by *Sleighter et al*. [2012]) within 10% RSD. After high reproducibility for the three samples was established, a molecular formula calculator generated empirical formula matches for all samples using carbon, hydrogen, oxygen, nitrogen, and sulfur with atomic ranges of $C_{5-50}H_{5-100}O_{1-30}N_{0-4}S_{0-2}$. Molecular formulas were assigned based on the rules described by *Stubbins et al*. [2010], and the calculated theoretical *m/z* values of the assigned formulas agreed with measured *m/z* values with an error value of ≤0.5 ppm. For all samples (including duplicate analyses), 78–85% of all peaks were assigned a unique molecular formula (excluding contributions from ^{13}C isotopes), and these formulas accounted for 84–92% of the summed total spectral peak magnitude.

2.4. Statistical Analysis

To understand how the groups of formulas classified here as labile, semilabile, and recalcitrant relate to the general compound classes identified via CDOM or FDOM analysis (e.g., terrigenous humic like or amino acid like), linear regressions and Spearman ranking were conducted on the optical and FTICR-MS data sets of the nine stream water samples (initial stream water plus eight bioreactor effluents). Linear regressions were performed between absorption coefficients (e.g., *a*305), CDOM proxies for molecular weight (spectral slope ratio S_R, ratios of long to short wavelength absorption by CDOM) [*Helms et al*., 2008], or FDOM fractions (humic- or amino acid-like FDOM) with groups of molecular formulas assigned to compound classes such as protein, lipid, or lignin [*Hockaday et al*., 2009; *Ohno et al*., 2010]. Correlations were determined to be significant for slopes significantly different than zero at the 95% confidence interval. Spearman ranking, a statistical measure of the dependence between two variables, was conducted similarly to that described by *Herzsprung et al*. [2012] and *Stubbins et al*. [2013] by relating CDOM absorption coefficients or FDOM fractions to the relative magnitudes for each of the molecular formulas that were found to be common to all nine samples in the data set (correlations were significant at an α level of $p \leq 0.05$).

Principal component analysis was conducted on the formula assignments to the nine samples analyzed by FTICR-MS. A data matrix was created for the samples and the complete set of unique formulas using the relative magnitudes of the peaks. Relative magnitude is simply calculated by dividing the peak magnitude by the summed total peak magnitude for each sample. If a formula was not detected in that sample, a 0 was given in the matrix. Using this matrix, principal component analysis (PCA) was conducted according to *Sleighter et al*. [2010]. The effluent from the bioreactor with an EBCT of 1.5 min was found to be an outlier during this analysis and was thus excluded; the PCA was then executed using the initial stream water and other seven bioreactor samples (including the duplicates, there were 11 samples total).

Two-dimensional correlation analysis (2-D correlation) was conducted according to *Abdulla et al*. [2013] on the formula assignments to the mass spectral peaks acquired for the nine DOM samples (for simplicity, one of each of the three duplicate analyses was utilized), using EBCT as the perturbation factor. Unlike PCA, 2-D correlation is based on the presence or absence of individual formulas, where each of the assigned CHO-only formulas within all nine van Krevelen diagrams was divided into two separate diagrams, one for H/C and one for O/C. In each case, the elemental ratio (either H/C or O/C on the *x* axis) was plotted against the total number of molecular formulas at each specific elemental ratio (on the *y* axis). The synchronous 2-D correlation was conducted on each of the H/C and O/C matrices as described in *Abdulla et al*. [2013].

3. Results and Discussion

3.1. DOC

The stream water DOC concentration decreased with increasing bioreactor residence time with a total loss of 45% of the initial DOC concentration (1.62 mg C/L) in 271.5 min (Figure 1 and Table 1). Effluent from the bioreactor with 271.5 min EBCT had a DOC concentration of 889 μg C/L and a BDOC of 729 μg C/L. These data, showing a 3% increase in %BDOC with a 1.8-fold increase in residence time, were used to fit the G-model of DOC concentration versus EBCT and separate the DOM from White Clay Creek into labile (237 μg C/L), semilabile (484 μg C/L), and recalcitrant (885 μg C/L) classes ($R^2 = 0.99$; $p < 0.0001$). The stream water was composed of 15% labile, 30% semilabile, and 55% recalcitrant DOC, meaning that 55% of the DOC pool passed through all bioreactors without being respired by microorganisms.

Using previously developed relationships to scale BDOM uptake in the bioreactors to uptake in White Clay Creek (via ^{13}C-DOM tracer additions) [*Kaplan et al*., 2008], we can generalize the meaning of the bioreactivity

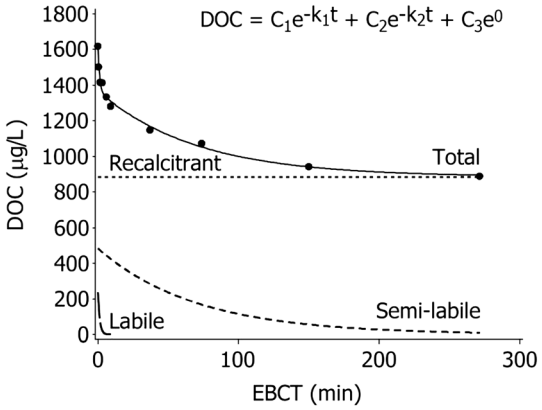

Figure 1. The measured dissolved organic carbon (DOC) concentrations after stream water was passed through a series of bioreactors with varying empty bed contact times (EBCTs) (corresponding to the data given in Table 1), along with the model results separating the DOC into labile, semilabile, and recalcitrant classes. Error bars from the standard deviations given in Table 1 are smaller than data points.

terms in relation to the fate of DOM molecules in a small headwater stream. Uptake lengths are influenced by depth, velocity, and biological demand for DOM and, thus, are specific for individual streams. Given that caveat, for White Clay Creek with typical baseflow discharge of 50–100 L/s, the labile DOM would have turnover times of hours, travel downstream a few hundred meters, and be metabolized within the reach where it originated; the semilabile DOM with a turnover time of days would travel out of the reach and be transported several kilometers downstream before being metabolized; and the more recalcitrant DOM with longer, but an unknown, turnover time flows through the river network without being metabolized [*Cory and Kaplan*, 2012]. The proportion (45%) of DOM that was biodegradable (i.e., the sum of labile and semilabile constituents) was 7% higher than previous measurements in White Clay Creek under base flow conditions [*Kim et al*., 2006], and the most bioreactive or labile proportion of the DOM was nearly 2 times higher [*Cory and Kaplan*, 2012; *McLaughlin and Kaplan*, 2013], presumably because the water was collected near the peak of autumn leaf fall and would likely contain higher concentrations of fresh, labile leaf leachate [*Sweeney*, 1993].

3.2. CDOM and FDOM

Stream water CDOM and FDOM concentrations decreased with increasing bioreactor residence time (i.e., EBCT), with total losses in the range of 24–87% of the initial CDOM or FDOM. The magnitude of loss of CDOM or FDOM varied with wavelength, corresponding to variations in lability of different CDOM and FDOM fractions to microorganisms. For example, the S_R (which is inversely related to molecular weight) decreased by 24% as a function of EBCT (Table 1), indicating a preferential removal of molecules with lower average molecular weight [*Helms et al*., 2008] compared to molecules not taken up by microorganisms. Humic-like FDOM components C1, C2, and C3 decreased by 31%, 43%, and 45%, respectively, while tryptophan-like FDOM (C4) decreased by 64% and tyrosine-like FDOM (C5) decreased by 87% (Figure 2, Table 1). These lability profiles of CDOM and FDOM are consistent with previous work in White Clay Creek on different dates showing preferential removal of low molecular weight CDOM and protein-like FDOM compared to larger molecular weight CDOM and humic-FDOM [*Cory and Kaplan*, 2012] and are consistent with direct

Table 1. The Measured Dissolved Organic Carbon (DOC) and Calculated Biodegradable DOC (BDOC) Concentrations After Stream Water was Passed Through a Series of Bioreactors With Varying Empty Bed Contact Times (EBCTs) (Corresponding to the Plot Given in Figure 1), Along With the Slope Ratio (S_R) [*Helms et al*., 2008] Calculated From the Absorbance Spectrum and the Fluorescent Dissolved Organic Matter (FDOM) Components Generated by PARAFAC Analysis for Each Sample (Corresponding to the Plot Given in Figure 2)

					FDOM (RU)				
Sample	EBCT (min)	DOC[a] (µg/L)	BDOC[a] (µg/L)	S_R	C1	C2	C3	C4	C5
Stream	0.0	1618 ± 26	0	0.756	0.255	0.137	0.119	0.131	0.019
K8-1	0.5	1502 ± 7	116 ± 27	0.739	0.252	0.130	0.110	0.079	0.026
K8-2	1.5	1417 ± 5	201 ± 26	0.700	0.239	0.126	0.112	0.067	0.024
K8-3	3.0	1415 ± 7	203 ± 27	0.634	0.232	0.115	0.094	0.052	0.014
K8-4	6.0	1335 ± 2	283 ± 26	0.703	0.224	0.106	0.086	0.046	0.011
K8-5	9.0	1282 ± 2	336 ± 26	0.625	0.218	0.113	0.096	0.049	0.011
K8-7	37.0	1148 ± 2	470 ± 26	0.621	0.196	0.094	0.077	0.054	0.014
K8-8	73.8	1073 ± 5	545 ± 26	0.561	0.185	0.085	0.071	0.048	0.012
K2-1	150.0	943 ± 5	676 ± 26	0.576	0.173	0.079	0.065	0.050	0.002

[a]Data are expressed as mean ± standard deviation ($n = 2$).

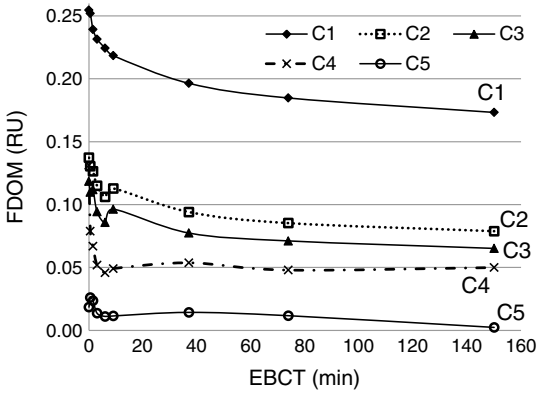

Figure 2. Fluorescent dissolved organic matter (FDOM) components generated by PARAFAC analysis for each of the bioreactor samples (corresponding to the data given in Table 1).

measurements of the uptake in bioreactors of amino acids and humic substances [*Volk et al*., 1997].

However, in contrast to previous investigations of FDOM biodegradability in White Clay Creek, here we observed nearly twofold greater loss of humic-like FDOM (31–45%) compared to previous bioreactor measurements that showed at most a 16% loss of humic-like FDOM components C1, C2, and C3 [*Cory and Kaplan*, 2013]. As mentioned above, we suggest this difference in lability of humic-like FDOM is associated with the timing of seasonal leaf fall and the likely presence of groups of molecules with similar fluorescence spectra but with a range of bioreactivities to microbial degradation. Our previous study sampled DOM lability in White Clay Creek in early October 2009 and May 2010 with little or no overlap with leaf litter senescence. Leaf litter contributes to humic-like FDOM [*Cuss and Guéguen*, 2012], and the fall in or blow in of fresh litter that bypasses processing in the soil is likely more labile than soil-derived FDOM that has been previously degraded by the soil microflora prior to export to the stream. Although a temporal analysis of lability profiles was beyond the scope of this investigation, different lability profiles within fractions of DOM (e.g., within the FDOM pool as observed in this example) support the dynamic nature of bioreactive DOM [*Fellman et al*., 2008, 2009a; *McLaughlin and Kaplan*, 2013] and point to the need for measurements designed to capture differences due to season and changes in hydrology during storms.

3.3. ESI-FTICR-MS

The FTICR mass spectra for the samples show high complexity, as expected from DOM, and thousands of molecular formulas were assigned for each sample. There were 38,640 formulas assigned to the peaks detected in all nine samples (including the replicate analyses), and when removing the duplicates (i.e., formulas assigned in more than one sample), a total of 5098 unique formulas existed. The spectra are similar to those presented in numerous studies of stream water DOM, with peaks detected at 200–700 m/z and up to 25 peaks per nominal mass [*Koch et al*., 2005; *Sleighter and Hatcher*, 2008; *Sleighter et al*., 2009; *Reemtsma*, 2009]. What is unique to this data set is the fact that a microbial degradation continuum is recorded by the disappearance and appearance of mass spectral peaks associated with the overall process taking place within the bioreactors. We can now use these specific molecular formulas in the DOM to identify the kinds of molecules associated with labile, semilabile, and recalcitrant DOM. Labile and semilabile DOM are molecules that were present in the original stream water but decreased with passage through the bioreactors so that the labile DOM was mostly removed with an EBCT of ≤3 min and not detected in effluents beyond an EBCT of 9 min, while the concentration of semilabile DOM approached zero with an EBCT of ≤150 min (Figure 1). Recalcitrant DOM corresponds to peaks that were either originally present in the stream water that persist over exposure times in the bioreactors or peaks that were augmented or were newly formed in passage through the bioreactors as the result of autochthonous production or excretion. We differentiate the latter as a new pool of DOM molecules. The various formulas associated with the four different pools of DOM over the course of biodegradation were identified and are discussed in detail below. In addition to compartmentalizing peaks/formulas on the basis of biodegradation reactivity, one can parse the formulas by regions of the van Krevelen diagram that denote molecular similarities with groups of compounds such as proteins, carbohydrates, lignin, or condensed aromatics [*Hockaday et al*., 2009; *Ohno et al*., 2010].

3.4. Relating CDOM, FDOM, and Molecular Formula Assignments

While studies have been conducted using both EEMs and FTICR-MS [*Gonsior et al*., 2009, 2011; *Herzsprung et al*., 2012; *Stubbins et al*., 2012], there remains a need to connect fluorescence and absorbance characteristics of DOM, approaches well suited to capture DOM dynamics over temporal scales characteristic of aquatic ecosystems, to the molecular composition of DOM that can be resolved by FTICR-MS. FTICR-MS provides

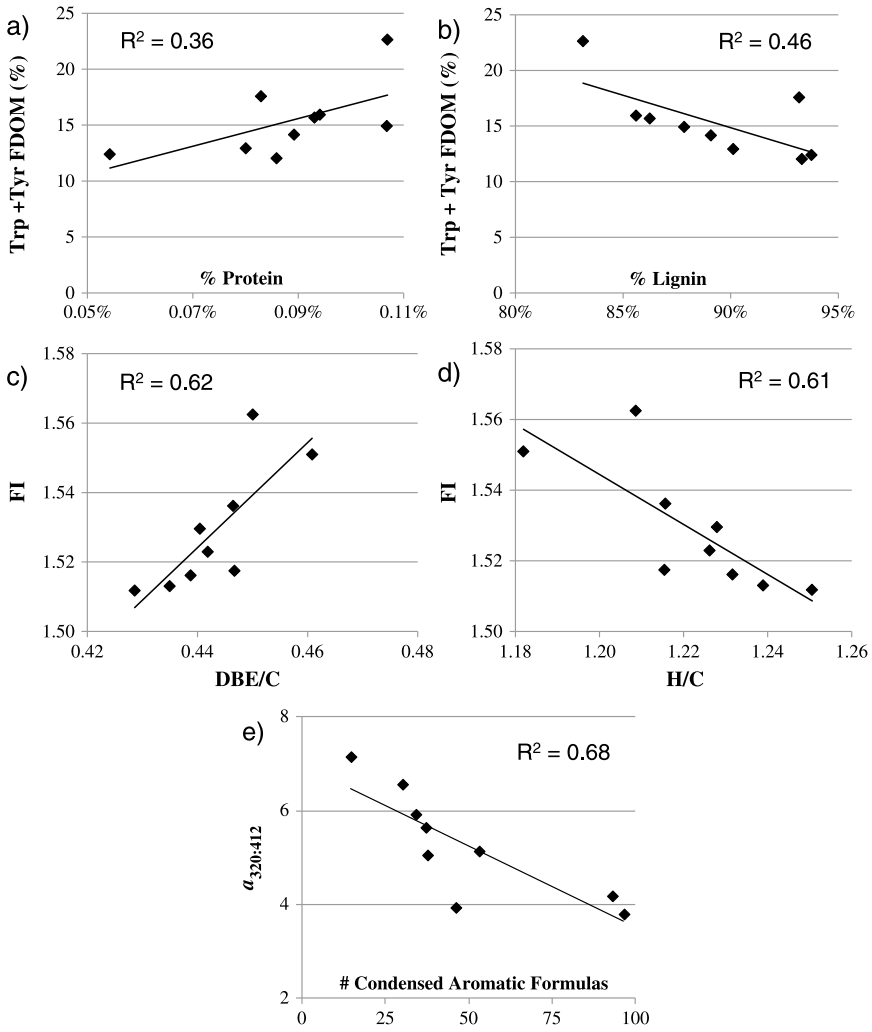

Figure 3. Relationships observed between EEMs analysis and FTICR-MS analysis, where the total amino acid-like FDOM (sum of tryptophan- and tyrosine-like FDOM) as a percent of the total FDOM was correlated with the percent of spectral magnitude attributed to the (a) protein-like (O/C 0.2–0.6, H/C 1.5–2.2, N/C ≥ 0.05) formulas and (b) lignin-like (O/C 0.1–0.6, H/C 0.6–1.7, $AI_{mod} < 0.67$, *Koch and Dittmar* [2006]) formulas; the fluorescence index (FI) is correlated with the number-averaged (c) DBE/C (double bond equivalents normalized to carbon) values and (d) H/C values; and the molar absorptivity ratio of 320:412 nm ($a_{320:412}$) is correlated with (e) the average *m/z* values and (f) the number of formulas classified as condensed aromatic (O/C 0.0–1.0, H/C 0.3–0.7, $AI_{mod} \geq 0.67$). Data shown here correspond with that presented in Table 2.

extremely rich molecular-level data and has great potential to refine our understanding of the major FDOM peaks. A number of significant correlations were identified between CDOM, FDOM, and groups of formulas assigned to compound classes. For example, the fraction of amino acid-like FDOM (sum of tryptophan- and tyrosine-like FDOM divided by total FDOM) was positively correlated with the percent spectral magnitude attributed to the protein-like formulas (O/C 0.2–0.6, H/C 1.5–2.2, N/C ≥ 0.05, $R^2 = 0.36$, $p < 0.05$; Figure 3a and Table 2). Although amino acid-like FDOM and protein-like formulas in the FTICR-MS analysis were both small fractions of the total respective signals, we expect these signals to exhibit similar dynamics in the bioreactors if they both are attributed to free or combined amino acid carbon. In contrast, while lipid-like formulas (O/C 0.0–0.2, H/C 1.7–2.2) were also a small fraction of the total FTICR-MS signals and also showed some variability in the bioreactors, there was no correlation between lipid-like signals and amino acid-like FDOM, suggesting that, as expected, these signals represent different types of carbon.

The fraction of amino acid-like FDOM was inversely correlated with the percent spectral magnitude attributed to lignin-like formulas (O/C 0.1–0.6, H/C 0.6–1.7, $AI_{mod} < 0.67$ [*Koch and Dittmar*, 2006] $R^2 = 0.46$, $p < 0.05$;

Table 2. Data Corresponding to That Presented in the Plots Shown in Figure 3, Highlighting the Relationships Observed Between EEMs Analysis and FTICR-MS Analysis

				FTICR-MS Data					
	Optical Data			% of Spectral Magnitude		Number of Formulas	Number Averaged		
Sample	Amino Acid-Like (% Total FDOM)	FI	$a_{320:412}$	Protein Like	Lignin Like	Condensed Aromatic	DBE/C	H/C	*m/z*
Stream	22.6%	1.56	3.81	0.11%	83%	97	0.45	1.21	445
K8-1	17.6%	1.53	3.94	0.08%	93%	46	0.44	1.23	449
K8-2	15.9%	1.55	4.19	0.09%	86%	93	0.46	1.18	441
K8-3	12.9%	1.51	5.93	0.08%	90%	34	0.43	1.25	451
K8-4	12.0%	1.52	5.06	0.09%	93%	38	0.44	1.23	451
K8-5	12.4%	1.54	5.65	0.05%	94%	37	0.45	1.22	455
K8-7	15.7%	1.52	5.15	0.09%	86%	53	0.45	1.22	447
K8-8	14.9%	1.52	6.57	0.11%	88%	30	0.44	1.23	450
K2-1	14.1%	1.51	7.16	0.09%	89%	15	0.43	1.24	454

Figure 3b and Table 2). A negative correlation between amino acid-like FDOM and the percent spectral magnitude attributed to lignin-like formulas indicates that these types of carbon exhibit opposite dynamics in the bioreactors and may suggest that as the more labile compounds are removed, compounds with chemical composition similar to that of lignin become more enriched in the stream water, consistent with the known relatively recalcitrant nature of lignin compared with amino acids [*Cowie and Hedges*, 1992].

Other correlations also suggest a consistency between the optical and FTICR-MS data. For instance, the fluorescence index (FI) was positively correlated with number-averaged double bond equivalents normalized to carbon (DBE/C, $R^2 = 0.62$, $p < 0.05$; Figure 3c and Table 2) and negatively correlated with number-averaged H/C ($R^2 = 0.61$, $p < 0.05$; Figure 3d and Table 2). FI, DBE/C, and H/C are each proxies for the aromatic C content of DOM, and FI values close to 1.2 indicate a more terrestrial source while FI values close to 1.8 indicate a more microbial source [*McKnight et al.*, 2001; *Sleighter and Hatcher*, 2008]. Because each proxy for aromatic C changed together and indicated an increase in aromatic C with increasing residence time as DOM was degraded by microorganisms in the bioreactors, it is likely that microbial heterotrophs preferentially removed the less aromatic C.

Ratios of CDOM absorbance at shorter to longer wavelength (e.g., the ratio of a_{320} to a_{412}) were negatively correlated with the number of formulas classified as condensed aromatic (O/C 0.0–1.0, H/C 0.3–0.7, $AI_{mod} \geq 0.67$, $R^2 = 0.68$, $p < 0.05$; Figure 3e and Table 2). This result is consistent with the expectation that condensed aromatics contribute to the absorption of CDOM at longer wavelengths and thus decrease the ratio of short to long wavelength absorption [*Chin et al.*, 1997].

While linear regressions between CDOM, FDOM, and groups of formulas assigned to a compound class demonstrate corroboration between optical and FTICR-MS data of labile and semilabile DOM and are consistent with the types of DOM expected to be susceptible to microbial degradation, stronger correlations between CDOM, FDOM, and peak magnitudes were observed for individual molecular formulas (e.g., those not grouped by compound class) using a Spearman Rank analysis [*Herzsprung et al.*, 2012; *Stubbins et al.*, 2013]. Between 4% and 16% of the formulas were significantly correlated to CDOM or FDOM ($R^2 \geq 0.6$; $p < 0.05$; Table 3). For example, a peak having *m/z* = 347.040856 ($C_{16}H_{11}O_9^-$, O/C = 0.56, H/C = 0.75) was significantly positively correlated with humic-like C1 fluorescence ($R^2 = 0.90$; $p = 0.0009$). Because CDOM and FDOM intensities decreased with increasing residence time due to microbial

Table 3. Number of Significant Correlations (as Determined by Spearman Rank Analysis) Between Optical and FTICR-MS Data Using the 1936 Formulas Common to All Nine Samples (Correlation Criteria = $p < 0.05$, $R^2 > 0.65$)

	CDOM	FDOM		
Optical Parameter	a_{305}	Humic C1	Tryptophan C4	Tyrosine C5
# of positive correlations (formulas removed by bacteria)	215 (11.1%)	206 (10.6%)	84 (4.3%)	179 (9.2%)
# of negative correlations (formulas resistant to bacterial degradation)	191 (9.9%)	181 (9.3%)	201 (10.4%)	309 (16.0%)

[a]The van Krevelen diagrams of these formulas are presented in Figure 4.

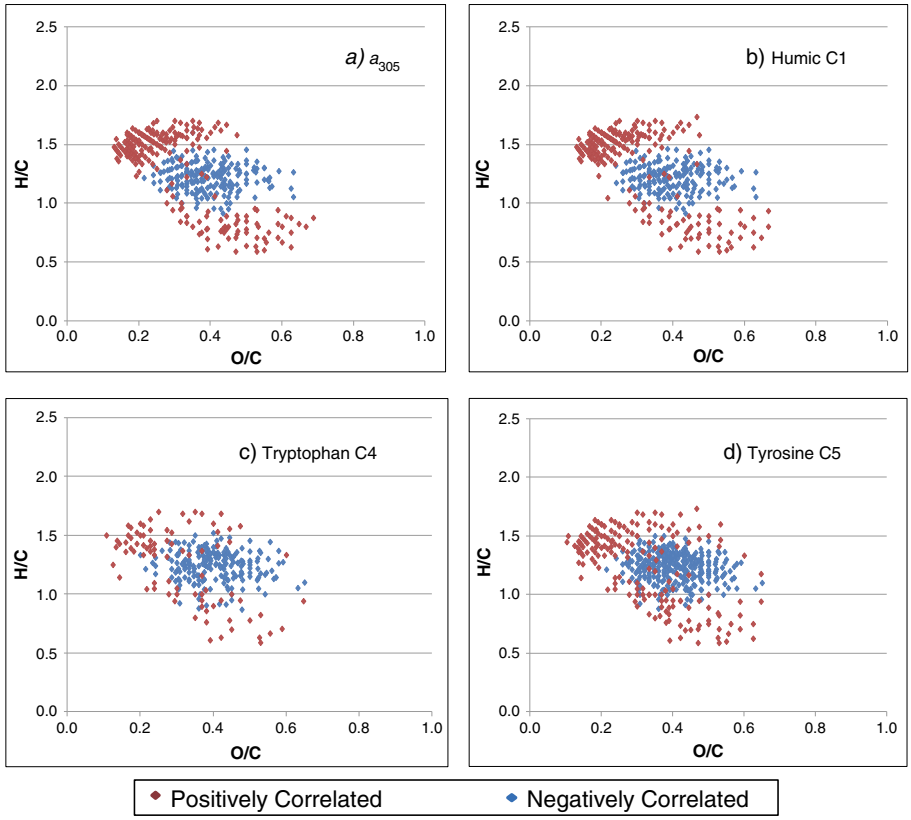

Figure 4. The van Krevelen diagrams of the formulas (based on their peak magnitudes for the nine samples) found to correlate significantly with either CDOM (a) a_{305} or FDOM, (b) humic C1, (c) tryptophan C4, and (d) tyrosine C5 during Spearman Rank analysis (Table 3). Only results meeting the correlation criteria are presented ($p < 0.05$, $R^2 > 0.65$), with red diamonds representing positive correlations (formulas removed by microorganisms) and blue diamonds representing negative correlations (formulas resistant to microbial degradation).

degradation, positive correlation with CDOM and FDOM revealed the formulas that were likely also removed by microbial degradation, while those negatively correlated with CDOM or FDOM are more recalcitrant. The van Krevelen diagrams of the formulas significantly correlated with CDOM or FDOM (Figure 4) showed that the formulas positively correlated with CDOM and FDOM consistently aligned in two regions: (1) formulas with H/C centered around 1.50 with O/C spanning 0.1–0.5 and (2) formulas with H/C ranging from 0.5 to 1.0 with O/C spanning 0.2–0.7. Given that these formulas were likely removed by microbial degradation in the bioreactors, compounds with these elemental characteristics were part of the labile or semilabile DOM pools.

Formulas negatively correlated with CDOM and FDOM consistently aligned in the middle of the van Krevelen diagram, covering an H/C range of 0.9–1.5 and O/C range of 0.25–0.65 (Figure 4). Negative correlations of formulas to CDOM and FDOM suggest that these formulas were preferentially enriched in the bioreactors with increasing residence time and were thus more recalcitrant to microbial degradation. These compounds may either increase in relative magnitude as other compounds are preferentially removed or they may be byproducts of microbial degradation. Compounds in this central region of the van Krevelen diagram are often those with the greatest relative magnitude in many aquatic systems. Our results suggest these compounds account for a large portion of the mass spectrum, perhaps because they accumulate in the environment as other compounds are preferentially degraded.

3.5. Multivariate Statistical Analyses

Multivariate statistical analysis reveals complementary information about DOM degradation within the bioreactors. Of the total 5098 unique formulas that were assigned to the samples based on FTICR-MS analysis (including those samples analyzed twice for reproducibility purposes), 1936 (or 38% of all formulas) were

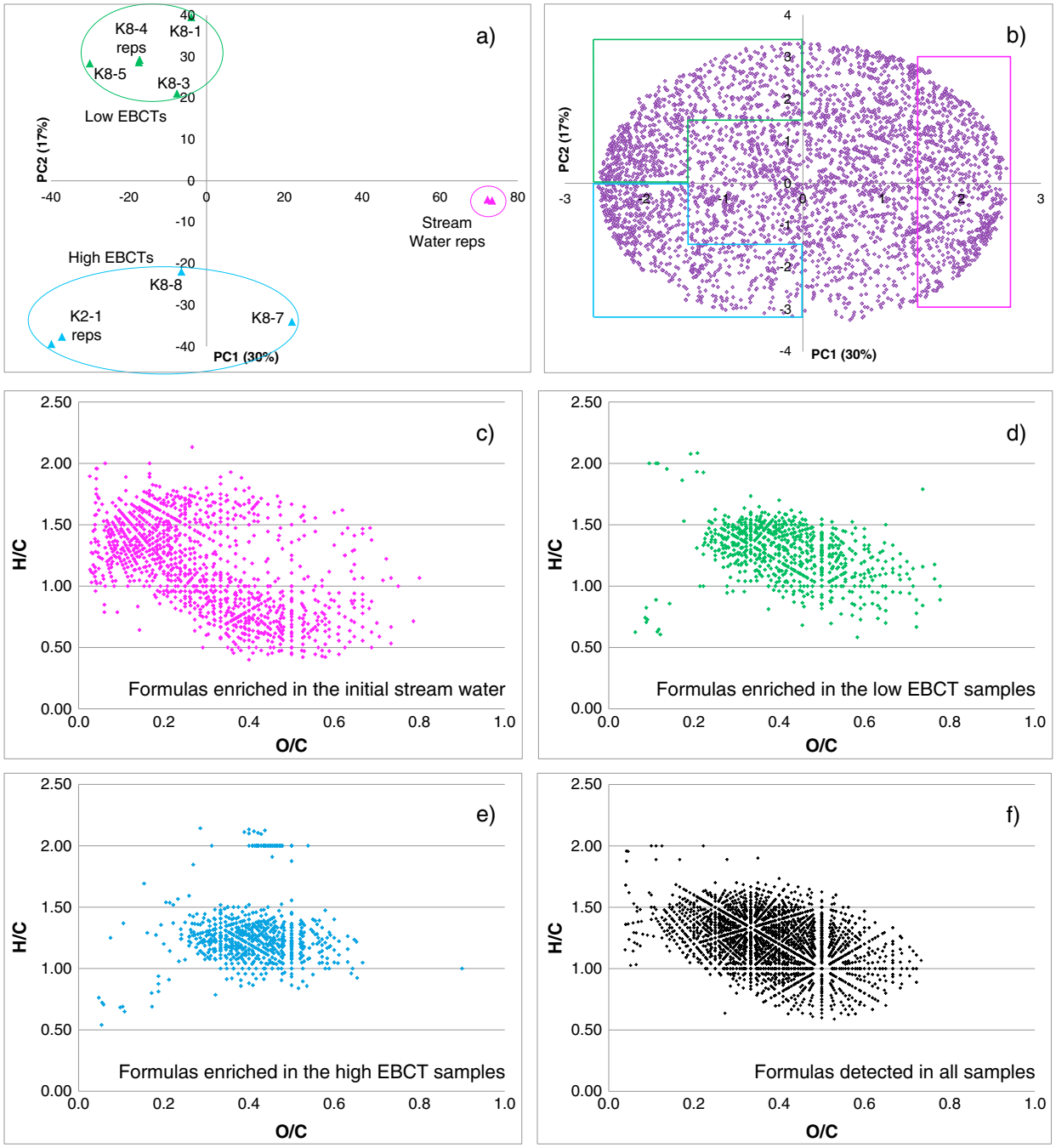

Figure 5. The principal component analysis (PCA) biplot of PC1 and PC2 showing the (a) samples' scores (i.e., the 11 FTICR-MS analyses that include instrumental duplicates) and (b) variables' loadings (i.e., the relative magnitude of the 5098 formulas). Formulas that fall into the colored boxes in Figure 5b that are enriched in the samples in the corresponding colored circles in Figure 5a are plotted on van Krevelen diagrams in Figures 5c–5e. Formulas that are detected in all 11 samples are plotted on the van Krevelen diagram in Figure 5f. Further characteristics of these four formula groupings are given in Table 4.

common to all samples, consistent with the majority of the DOC pool (55%) classified as recalcitrant to microbial degradation by our measurements. In order to better understand the fractions of DOC comprising the labile and semilabile categories, PCA was utilized to categorize these compounds based on the variability of the relative magnitudes of their assigned formulas across the mass spectral data set. The PCA biplot of PC1 and PC2 accounted for 47% of the total variance in the data set (Figures 5a and 5b). The PCA analysis separated the stream water along PC1, where the initial stream water had a very high positive PC1 score and

Table 4. Characteristics of the Four Formula Groupings Plotted on the van Krevelen Diagrams Presented in Figure 5

	General Characteristics of Formulas							
	Pink (Enriched in Inflow Water)		Green (Enriched in First Bioreactors)		Blue (Enriched in Final Bioreactors and Effluent)		Formulas in All Samples	
Parameter	Range	Average	Range	Average	Range	Average	Range	Average
O/C	0.03–0.80	0.30	0.06–0.78	0.42	0.05–0.67[a]	0.41	0.04–0.73	0.38
H/C	0.40–2.13	1.15	0.58–2.08	1.27	0.54–2.14	1.27	0.59–2.00	1.23
DBE	0–24	10.76	0–25	9.91	0–28	10.23	1–20	9.86
DBE/C	0.0–0.86	0.48	0.0–0.75	0.42	0.0–0.76	0.42	0.05–0.76	0.44
m/z	219–679	413.98	271–689	484.59	285–689[b]	488.90	245–671	444.09
C#	13–47	23.07	13–37	24.20	13–42	24.47	14–39	22.81
%CHO	73%		67%		55%		67%	
%CHON	22%		26%		37%		27%	
%CHOS	5%		7%		8%		6%	

[a]Exception: One formula with O/C 0.90.
[b]Exception: One formula with *m/z* 209.

the stream water effluent (after the bioreactors) had either a low positive PC1 score or a negative PC1 score (Figure 5a). PC2 separated the stream water as a function of residence time (EBCT). Stream water DOM samples with low EBCTs (≤9 min, the labile fraction) have high positive PC2 scores, while samples with higher EBCTs (>9 min, the semilabile and recalcitrant fractions) have high negative PC2 scores (Figure 5a).

By combining the locations of the scores of the samples (Figure 5a) with the loadings of the variables (Figure 5b), we can further examine the formulas that are thus enriched in the various samples and then plot them on the van Krevelen diagram to examine the compositional differences (Figures 5c–5e and Table 4). Examining the characteristics of the stream water DOM with high positive PC1 scores and loadings, it is evident that these formulas, enriched in the initial stream water (those with PC1 > 1.5, Figure 5b pink box) and representing the labile compounds, plot with a wide distribution in van Krevelen space but clearly lack points in the center of the plot (Figure 5c). The composition of these formulas labile to biodegradation were 73% CHO, 22% CHON, and 5% CHOS (Table 4), and they accounted for over 20% of the total spectral magnitude in the original stream water (Table 5) but decreased significantly after passing through the first bioreactors (those with short residence time). Stream water DOM after bioreactors with low EBCTs have negative PC1 scores and positive PC2 scores and were enriched in the formulas of the same characteristics [green box in Figure 5b; 67% CHO, 26% CHON, and 7% CHOS (Table 4)] but occupied the center region of the van Krevelen diagram (Figure 5d). Because these formulas were enriched in the DOM in the effluent of the bioreactors with low EBCTs, they represent semilabile DOM.

Stream water DOM in the effluent of the high EBCT bioreactors are enriched in formulas having negative PC1 and PC2 scores (blue box in Figure 5b), which accounted for increasing percentages of the total spectral

Table 5. The Percentage of Total Spectral Magnitude That is Accounted for by Each of the Four Formula Groupings Described in Table 4 and Presented in Figure 5

	Percentage of Total Spectral Magnitude			
Sample	Pink Formulas	Green Formulas	Blue Formulas	Formulas in All Samples
Stream (1)	21.2%	16.3%	20.5%	34.5%
Stream (2)	21.2%	16.2%	20.5%	34.7%
K8-1	13.8%	23.7%	25.2%	29.3%
K8-3	13.4%	22.2%	26.0%	28.9%
K8-4 (1)	12.6%	24.1%	26.2%	28.2%
K8-4 (2)	12.5%	24.3%	26.1%	29.0%
K8-5	11.5%	25.0%	27.0%	26.8%
K8-7	16.5%	17.6%	25.1%	33.0%
K8-8	14.0%	20.0%	26.5%	31.0%
K2-1 (1)	11.1%	20.8%	32.2%	28.4%
K2-1 (2)	11.3%	21.2%	31.2%	29.8%

Stream water, K8-4, and K2-1 were analyzed in duplicate.

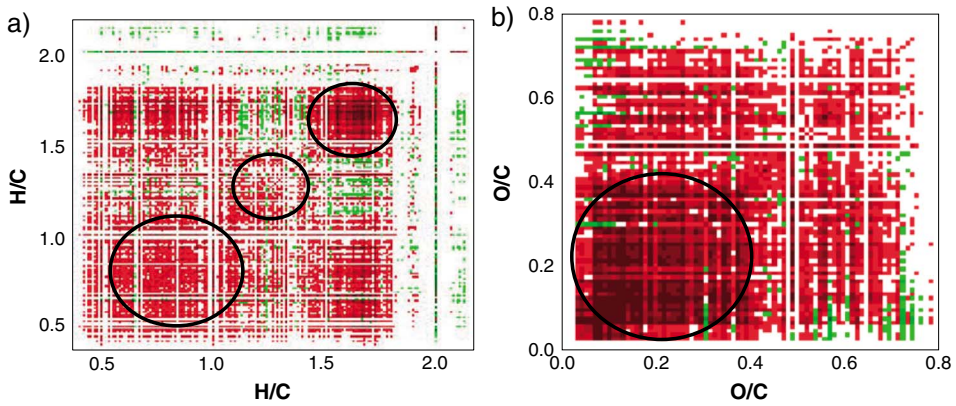

Figure 6. The synchronous maps generated from the presence or absence of individual formulas associated with the CHO-only molecular formulas assigned for the nine DOM samples using EBCT as the perturbation factor, displaying (a) H/C and (b) O/C each correlated with itself. Red signifies positive correlations while green denotes negative correlations, and higher color intensity indicates a stronger correlation. Black circles highlight areas of particular interest.

magnitude as the water passes through the bioreactors (Table 5). The formulas of this more recalcitrant class of DOM exhibited an even more narrow distribution in van Krevelen space (Figure 5e) and contained a small cluster of formulas with high H/C that spanned O/C 0.4–0.6. These formulas were 55% CHO, 37% CHON, and 8% CHOS (Table 4). Comparing the elemental composition among labile, semilabile, and more recalcitrant DOM, there was an increase in the relative magnitude of heteroatom-containing formulas (those containing N and S). This may be because microbial heterotrophs preferentially remove CHO-only formulas or because N and S containing formulas were byproducts of microbial degradation and thus increased in relative magnitude as EBCT increased.

Comparing the composition of the labile, semilabile, and more recalcitrant categories of DOM revealed by the PCA to the elemental composition of formulas common to all of the DOM samples may provide deeper insights into the more recalcitrant compounds, assuming that recalcitrant compounds were present in the initial stream water and in the effluent of each bioreactor (Figure 5f). The formulas common to all DOM classes decreased in relative magnitude with increasing residence time in the bioreactors (Table 5) and had elemental composition similar to labile and semilabile DOM (67% CHO, 27% CHON, and 6% CHOS; Table 4). Thus, these formulas common to all samples are likely less recalcitrant (more biodegradable) than the PCA-identified recalcitrant formulas (those exhibiting distinct elemental composition), because while the common formulas must persist through all the bioreactors (to be in the "common" subset of all detected formulas), they decreased in relative magnitude, likely due to progressive microbial degradation. In contrast, the pool of recalcitrant DOM identified above (blue formulas in Figures 5b and 5e) increased in relative magnitude as the water progressed through the bioreactors, possibly as labile and semilabile DOM were removed, thus enhancing these signals. Regardless of the degree to which the relative versus absolute increase in these more recalcitrant signals, both the PCA and Spearman analysis identified the more recalcitrant subset of the DOM pool as those compounds characterized by a narrow distribution of O/C and H/C ratios that tightly cluster in the central region of the van Krevelen plot (Figure 4).

By examining the presence or absence of individual formulas, we observed a significant decrease in the total number of CHO-only formulas with increasing EBCT, starting with 2396 individual CHO formulas in the stream water and ending with 1860 individual CHO formulas after 150 min EBCT. To highlight the areas on the van Krevelen diagrams that had the largest changes in the number of CHO formulas and examine the correlation between these areas, we used 2-D correlation as another statistical tool that has proven to be valuable for delineating groups of formulas associated with each other. Figure 6 shows the synchronous maps for the H/C and O/C plots (each correlated with themselves), where red indicates positive correlations (i.e., formulas changing in the same direction) and green indicates negative correlations (formulas changing in opposite directions). In Figure 6a, there are three key areas of interest, as indicated by the black overlain circles. Formulas at high H/C ratios of 1.5–1.8 show the greatest changes in the number of CHO formulas along EBCT, as indicated by the dominance of dark red coloring; followed by formulas at H/C ratios of 0.6–1.1, while the formulas at H/C

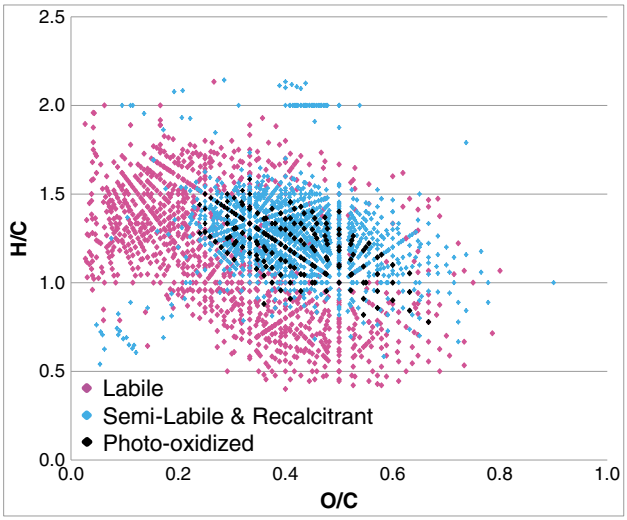

Figure 7. van Krevelen diagram highlighting the overlap between formulas classified as semilabile and recalcitrant (those in Figures 5d and 5e) with products of photooxidation of Suwannee River and/or Pony Lake fulvic acids in *Cory et al.* [2010b].

ratios of 1.1–1.5 show small changes relative to the formulas in the other two areas. Formulas at high H/C ratios of 1.5–1.8 are positively correlated with formulas at low H/C ratios (0.6–1.1), as indicated by the red coloring of these groups at the off-diagonal, meaning that these two groups of formulas are changing together. As previously discussed above from the Spearman Ranking and PCA, these two regions are associated with DOM that is labile or semilabile and degraded by microbial heterotrophs (Figures 4 and 5c). In contrast, formulas more central to the van Krevelen diagram with H/C 1.1–1.5 are negatively correlated with formulas with high H/C (1.5–1.8), as indicated by the off-diagonal green coloring in Figure 6a, which indicates that this group of formulas at H/C 1.1–1.5 is changing in the opposite direction to the other two groups (H/C 1.5–1.8 and 0.6–1.1) as EBCT increases. This observation is consistent with the more recalcitrant DOM described above that aligns in the middle of the van Krevelen plot (Figures 4 and 5e). Figure 6b shows the correlation of O/C ratios, and formulas with low O/C ($<$0.4) are changing the most, as signified by the dark red color intensity that is circled. This suggests that the low O/C formulas are most labile and likely to be degraded rather quickly, as also highlighted by the high presence of these types of formulas in Figure 5c of the initial stream water that is most quickly lost after being exposed to bioreactors with low EBCTs.

The high consistency of the three different statistical methods (Spearman ranking, PCA, and 2-D correlation) utilized here is very encouraging, as all three methods were executed independently of each other but essentially demonstrate the same trends between the various samples, thus corroborating each other. The utility of using these various tools together highlights the success of our approach designed here to elucidate the biological reactivity of molecules present in stream waters, by relating DOM optical properties to molecular composition and reactivity. It is important to note that these analyses allow us to assemble lists of molecular formulas belonging to the three subclasses of biodegradation, a capability that makes a major stride toward molecular-level classification of the relative biodegradability of DOM components in stream waters.

4. Conclusions

Taken together the bulk DOC analysis of the bioreactivity fractions of DOM combined with the analysis of DOM chemical composition via CDOM, FDOM, and FTICR-MS, we showed that in White Clay Creek stream water collected at the time of leaf fall, 45% of the DOC could be considered labile or semilabile. We suggest that the majority of the BDOC was humic DOM, based on reductions in the CDOM and humic-like FDOM constituents that were similar to the overall DOC reduction and the knowledge that humic substances account for most of the stream water DOC, CDOM, and FDOM. Additional support for this suggestion comes from the correlations between CDOM, FDOM, and molecular formulas that revealed the humic-like FDOM possessed characteristics consistent with DOM susceptible to biodegradation. Under the study conditions, BDOM was poor in heteroatom content and occupied distinct regions of van Krevelen space [low O/C compounds ($<$0.4) with H/C $>$ 1.5 and lower H/C compounds ($<$1.0) spanning an O/C range of approximately 0.2–0.6]. Compounds more recalcitrant to degradation in this study primarily were centered in van Krevelen space with median H/C and O/C ratios of about 1.25 and 0.45, respectively. The shrinking of the molecular cloud within the van Krevelen diagram with increasing bioreactor residence time (i.e., EBCT) and clear PCA separation of these molecular pools is striking. Interestingly, the elemental composition and van Krevelen space occupied by these more recalcitrant compounds overlaps well with oxidized DOM compounds

produced by photochemical reactions of CDOM [*Cory et al*., 2010b]. Of the 167 unique molecular formulas produced by photochemical oxidation of Suwannee River and/or Pony Lake fulvic acids, 112 (67%) were also found to exist in the group of formulas classified here as semilabile and/or recalcitrant (Figure 7). It is expected that these photooxidized products are less labile to microorganisms, and consistently, photoreacted Suwannee River and Pony Lake fulvic acids (representing terrestrial and aquatic end-members, respectively) showed slower bacterial growth rates when compared to unreacted controls [*Cory et al*., 2010b]. The overlap of these photoproducts with recalcitrant DOM suggests a similarity between oxidation end-points arrived at through separate mechanisms: biological oxidation and photooxidation, perhaps indicating that photodegradation of DOM produces compounds that bacteria are unable to use. This is consistent with many studies showing that photodegradation of DOM can negatively impact its lability to microbial degradation, depending on the source and composition of DOM [*Tranvik and Bertilsson*, 2001; *Cory et al*., 2010b, 2013].

Our analyses are based on a single sample collected from White Clay Creek likely associated with peak leaf fall, so we hesitate to extrapolate these results to a generalized model of biological reactivity classes. However, it is useful to compare our observations with other research that has utilized DOM distribution in van Krevelen space to identify the characteristics of bioreactive DOM. Previous studies of BDOM in temperate or tropical streams and rivers reported different distributions of formulas labile to microbial degradation than the distribution observed in this study. For example, even though *Kim et al*. [2006] showed that microbial degradation by stream heterotrophs consumed some of the low molecular weight compounds and oxygen-rich compounds that we also observed in this study, they found that microbial degradation generally modified the DOM pool toward lower molecular weight, oxygen-poor molecules. *Ward et al*. [2013] observed degradation of lignin and phenolic compounds that aligned in the center of the van Krevelen diagram, overlapping with the H/C and O/C ratios of the formulas identified as semilabile or more recalcitrant in this study. Together, these studies support the variable and dynamic nature of bioreactive DOM and demonstrate that the chemical composition of the more abundant bioreactive humic pool does not neatly align with our expectations of bioreactivity. These disparities also point to a limitation of our present analytical window, as the FTICR-MS approach provides composition of DOM but not structure, and chemical structure is clearly an important attribute that affects bioreactivity. Nevertheless, this study represents an important advancement, as we have demonstrated that our approach of FTICR-MS analysis of DOM after bioreactors varying by their EBCT, in combination with multivariate statistical analysis, allows for precise, robust analysis of compound bioreactivity and associated composition that if broadly applied may help develop a generalized model of biological reactivity classes. Correlations between optical properties and molecular properties of DOC along a bioreactivity gradient supported the use of FDOM to follow temporal dynamics of DOM, which is critical because it is not yet feasible to use FTICR-MS to capture the often rapid dynamics of DOM quantity and quality in streams and river ecosystems [*Fellman et al*., 2010; *Cory and Kaplan*, 2012].

Acknowledgments

We thank the College of Sciences Major Instrumentation Cluster (ODU) for their assistance with mass spectral acquisition, S. L. Roberts (Stroud Center) for operation of bioreactors, and M. D. Gentile (Stroud Center) for analyses of DOC. Research of R. M. Cory was supported by NSF OPP-1023270. Research of L. A. Kaplan was supported by NSF DEB-1052716 and EAR-0724971. Data used to produce the results of this paper can be obtained by contacting R.L.S.

References

Abdulla, H. A. N., R. L. Sleighter, and P. G. Hatcher (2013), Two dimensional correlation analysis of Fourier transform ion cyclotron resonance mass spectra of dissolved organic matter: A new graphical analysis of trends, *Anal. Chem.*, *85*(8), 3895–3902, doi:10.1021/ac303221j.

Aiken, G. R., D. M. McKnight, K. A. Thorn, and E. M. Thurman (1992), Isolation of hydrophilic organic acids from water using nonionic macroporous resins, *Org. Geochem.*, *18*(4), 567–573, doi:10.1016/0146-6380(92)90119-I.

Aufdenkampe, A. K., E. Mayorga, P. A. Raymond, J. M. Melack, S. C. Doney, S. R. Alin, R. E. Aalto, and K. Yoo (2011), Riverine coupling of biogeochemical cycles between land, oceans, and atmosphere, *Front. Ecol. Environ.*, *9*(1), 53–60, doi:10.1890/100014.

Balcarczyk, K. L., J. B. Jones Jr., R. Jaffé, and N. Maie (2009), Stream dissolved organic matter bioavailability and composition in watersheds underlain with discontinuous permafrost, *Biogeochemistry*, *94*(3), 255–270, doi:10.1007/s10533-009-9324-x.

Battin, T. J., L. A. Kaplan, S. Findlay, C. S. Hopkinson, E. Marti, A. I. Packman, J. D. Newbold, and F. Sabater (2008), Biophysical controls on organic carbon fluxes in fluvial networks, *Nat. Geosci.*, *1*(2), 95–100, doi:10.1038/ngeo101.

Battin, T. J., S. Luyssaert, L. A. Kaplan, A. K. Aufdenkampe, A. Richter, and L. J. Tranvik (2009), The boundless carbon cycle, *Nat. Geosci.*, *2*(9), 598–600, doi:10.1038/ngeo618.

Benner, R. (2003), Molecular indicators of the bioavailability of dissolved organic matter, in *Aquatic Ecosystems—Interactivity of Dissolved Organic Matter*, edited by S. E. G. Findlay and R. L. Sinsabaugh, pp. 121–138, Academic Press, San Diego.

Carlson, C. A. (2002), Production and comsumption processes, in *Biogeochemistry of Marine Dissolved Organic Matter*, edited by D. A. Hansell and C. A. Carlson, pp. 91–151, Academic Press, San Diego.

Chin, Y.-P., G. R. Aiken, and K. M. Danielsen (1997), Binding of pyrene to aquatic and commercial humic substances: The role of molecular weight and aromaticity, *Environ. Sci. Technol.*, *31*(6), 1630–1635, doi:10.1021/es960404k.

Cleveland, C. C., J. C. Neff, A. R. Townsend, and E. Hood (2004), Composition, dynamics, and fate of leached dissolved organic matter in terrestrial ecosystems: Results from a decomposition experiment, *Ecosystems*, *7*(3), 175–285, doi:10.1007/s10021-003-0236-7.

Coble, P. G. (1996), Characterization of marine and terrestrial DOM in seawater using excitation-emission matrix spectroscopy, *Mar. Chem.*, *51*(4), 325–346, doi:10.1016/0304-4203(95)00062-3.

Cole, J. J., and N. F. Caraco (2001), Carbon in catchments: Connecting terrestrial carbon losses with aquatic metabolism, *Mar. Freshwater Res.*, *52*(1), 101–110, doi:10.1071/MF00084.

Cole, J. J., et al. (2007), Plumbing the global carbon cycle: Integrating inland waters into the terrestrial carbon budget, *Ecosystems*, *10*(1), 172–185, doi:10.1007/s10021-006-9013-8.

Cory, R. M., and L. A. Kaplan (2012), Biological lability of streamwater fluorescent dissolved organic matter, *Limnol. Oceanogr.*, *57*(5), 1347–1360, doi:10.4319/lo.2012.57.5.1347.

Cory, R. M., and L. A. Kaplan (2013), Erratum: Biological lability of streamwater fluorescent dissolved organic matter, *Limnol. Oceanogr.*, *58*(1), 428, doi:10.4319/lo.2013.58.1.0428.

Cory, R. M., and D. M. McKnight (2005), Fluorescence spectroscopy reveals ubiquitous presence of oxidized and reduced quinones in dissolved organic matter, *Environ. Sci. Technol.*, *39*(21), 8142–8149, doi:10.1021/es0506962.

Cory, R. M., D. M. McKnight, Y.-P. Chin, P. Miller, and C. L. Jaros (2007), Chemical characteristics of fulvic acids from Arctic surface waters: Microbial contributions and photochemical transformations, *J. Geophys. Res.*, *112*, G04S51, doi:10.1029/2006JG000343.

Cory, R. M., M. P. Miller, D. M. McKnight, J. J. Guerard, and P. L. Miller (2010a), Effect of instrument-specific response on the analysis of fulvic acid fluorescence spectra, *Limnol. Oceanogr.: Methods*, *8*, 67–78, doi:10.4319/lom.2010.8.67.

Cory, R. M., K. McNeill, J. P. Cotner, A. Amado, J. M. Purcell, and A. G. Marshall (2010b), Singlet oxygen in the coupled photochemical and biochemical oxidation of dissolved organic matter, *Environ. Sci. Technol.*, *44*(10), 3683–3689.

Cory, R. M., B. C. Crump, J. A. Dobkowski, and G. W. Kling (2013), Surface exposure to sunlight stimulates CO_2 release from permafrost soil carbon in the Arctic, *Proc. Natl. Acad. Sci. U.S.A.*, *110*(9), 3429–3434, doi:10.1073/pnas.1214104110.

Cowie, G. L., and J. I. Hedges (1992), Sources and reactivities of amino acids in a coastal marine environment, *Limnol. Oceanogr.*, *37*(4), 703–724.

Cummins, K. W., J. J. Klug, R. G. Wetzel, R. C. Petersen, K. F. Suberkropp, B. A. Manny, J. C. Wuycheck, and F. O. Howard (1972), Organic enrichment with leaf leachate in experimental lotic ecosystems, *BioScience*, *22*(12), 719–722, stable URL: http://www.jstor.org/stable/1296289.

Cuss, C. W., and C. Guéguen (2012), Impacts of microbial activity on the optical and copper-binding properties of leaf-litter leachate, *Front. Microbiol.*, *3*(166), 1–10, doi:10.3389/fmicb.2012.00166.

del Vecchio, R., and N. V. Blough (2004), On the origin of the optical properties of humic substances, *Environ. Sci. Technol.*, *38*(14), 3885–3891, doi:10.1021/es049912h.

Dittmar, T., B. Koch, N. Hertkorn, and G. Kattner (2008), A simple and efficient method for the solid phase extraction of dissolved organic matter (SPE-DOM) from seawater, *Limnol. Oceanogr.: Methods*, *6*, 230–235, doi:10.4319/lom.2008.6.230.

Fellman, J. B., D. V. D'Amore, E. Hood, and R. D. Boone (2008), Fluorescence characteristics and biodegradability of dissolved organic matter in forest and wetland soils from coastal temperate watersheds in southeast Alaska, *Biogeochemistry*, *88*(2), 169–184, doi:10.1007/s10533-008-9203-x.

Fellman, J. B., E. Hood, R. T. Edwards, and D. V. D'Amore (2009a), Changes in the concentration, biodegradability, and fluorescent properties of dissolved organic matter during stormflows in coastal temperate watersheds, *J. Geophys. Res.*, *114*, G01021, doi:10.1029/2008JG000790.

Fellman, J. B., E. Hood, D. V. D'Amore, R. T. Edwards, and D. White (2009b), Seasonal changes in the chemical quality and biodegradability of dissolved organic matter exported from soils to streams in coastal temperate rainforest watersheds, *Biogeochemistry*, *95*(2–3), 277–293, doi:10.1007/s10533-009-9336-6.

Fellman, J. B., R. G. M. Spencer, P. J. Hernes, R. T. Edwards, D. V. D'Amore, and E. Hood (2010), The impact of glacier runoff on the biodegradability and biochemical composition of terrigenous dissolved organic matter in near-shore marine ecosystems, *Mar. Chem.*, *121*(1–4), 112–122, doi:10.1016/j.marchem.2010.03.009.

Frazier, S. W., L. A. Kaplan, and P. G. Hatcher (2005), Molecular characterization of biodegradable dissolved organic matter using bioreactors and [$^{12}C/^{13}C$] tetramethylammonium hydroxide thermochemolysis GC-MS, *Environ. Sci. Technol.*, *39*(6), 1479–1491, doi:10.1021/es0494959.

Gonsior, M., B. M. Peake, W. T. Cooper, D. Podgorski, J. D'Andrilli, and W. J. Cooper (2009), Photochemically induced changes in dissolved organic matter identified by ultrahigh resolution Fourier transform ion cyclotron resonance mass spectrometry, *Environ. Sci. Technol.*, *43*(3), 698–703, doi:10.1021/es8022804.

Gonsior, M., B. M. Peake, W. T. Cooper, D. C. Podgorski, J. D'Andrilli, T. Dittmar, and W. J. Cooper (2011), Characterization of dissolved organic matter across the Subtropical Convergence off the South Island, New Zealand, *Mar. Chem.*, *123*(1–4), 99–110, doi:10.1016/j.marchem.2010.10.004.

Grace, J., and Y. Malhi (2002), Global change: Carbon dioxide goes with the flow, *Nature*, *416*(6881), 594, doi:10.1038/416594b.

Guillemette, F., and P. A. del Giorgio (2011), Reconstructing the various facets of dissolved organic carbon bioavailability in freshwater ecosystems, *Limnol. Oceanogr.*, *56*(2), 734–748, doi:10.4319/lo.2011.56.2.0734.

Helms, J. R., A. Stubbins, J. D. Ritchie, E. C. Minor, D. J. Kieber, and K. Mopper (2008), Absorption spectral slopes and slope ratios as indicators of molecular weight, source, and photobleaching of chromophoric dissolved organic matter, *Limnol. Oceanogr.*, *53*(3), 955–969, doi:10.4319/lo.2008.53.3.0955.

Hernes, P. J., B. A. Bergamaschi, R. S. Eckard, and R. G. M. Spencer (2009), Fluorescence-based proxies for lignin in freshwater dissolved organic matter, *J. Geophys. Res.*, *114*, G00F03, doi:10.1029/2009JG000938.

Herzsprung, P., W. von Tümpling, N. Hertkorn, M. Harir, O. Büttner, J. Bravidor, K. Friese, and P. Schmitt-Kopplin (2012), Variations of DOM quality in inflows of a drinking water reservoir: Linking of van Krevelen diagrams with EEMF spectra by rank correlation, *Environ. Sci. Technol.*, *46*(10), 5511–5518, doi:10.1021/es300345c.

Hockaday, W. C., J. M. Purcell, A. G. Marshall, J. A. Baldock, and P. G. Hatcher (2009), Electrospray and photoionization mass spectrometry for the characterization of organic matter in natural waters: A qualitative assessment, *Limnol. Oceanogr.: Methods*, *7*, 81–95, doi:10.4319/lom.2009.7.81.

Hood, E., J. Fellman, R. G. M. Spencer, P. J. Hernes, R. Edwards, D. D'Amore, and D. Scott (2009), Glaciers as a source of ancient and labile organic matter to the marine environment, *Nature*, *462*(7276), 1044–1047, doi:10.1038/nature08580.

Hopkinson, C. S., et al. (1998), Terrestrial inputs of organic matter to coastal ecosystems: An intercomparison of chemical characteristics and bioavailability, *Biogeochemistry*, *43*(3), 211–234, doi:10.1023/A:1006016030299.

Kaplan, L. A., and J. D. Newbold (1993), Biogeochemistry of dissolved organic carbon entering streams, in *Aquatic Microbiology- An Ecological Approach*, edited by T. E. Ford, pp. 139–165, Blackwell Scientific, Cambridge, U. K.

Kaplan, L. A., and J. D. Newbold (1995), Measurement of streamwater biodegradable dissolved organic carbon with a plug-flow bioreactor, *Water Res.*, *29*(12), 2696–2706, doi:10.1016/0043-1354(95)00135-8.

Kaplan, L. A., and J. D. Newbold (2003), The role of monomers in stream ecosystem metabolism, in *Aquatic Ecosystems—Interactivity of Dissolved Organic Matter*, edited by S. E. G. Findlay and R. L. Sinsabaugh, pp. 97–119, Academic Press, San Diego.

Kaplan, L. A., T. N. Wiegner, J. D. Newbold, P. H. Ostrom, and H. Gandhi (2008), Untangling the complex issue of dissolved organic carbon uptake: A stable isotope approach, *Freshwater Biol.*, *53*(5), 855–864, doi:10.1111/j.1365-2427.2007.01941.x.

Kim, S., L. A. Kaplan, and P. G. Hatcher (2006), Biodegradable dissolved organic matter in a temperate and a tropical stream determined from ultra-high resolution mass spectrometry, *Limnol. Oceanogr.*, *51*(2), 1054–1063, doi:10.4319/lo.2006.51.2.1054.

Kirchman, D. L. (2003), The contribution of monomers and other low molecular weight compounds to the flux of dissolved organic matter in aquatic ecosystems, in *Aquatic Ecosystems—Interactivity of Dissolved Organic Matter*, edited by S. E. G. Findlay and R. L. Sinsabaugh, pp. 218–241, Academic Press, San Diego.

Koch, B. P., and T. Dittmar (2006), From mass to structure: An aromaticity index for high-resolution mass data of natural organic matter, *Rapid Commun. Mass Spectrom.*, *20*(5), 926–932, doi:10.1002/rcm.2386.

Koch, B. P., M. Witt, R. Engbrodt, T. Dittmar, and G. Kattner (2005), Molecular formulae of marine and terrigenous dissolved organic matter detected by electrospray ionization Fourier transform ion cyclotron resonance mass spectrometry, *Geochim. Cosmochim. Acta*, *69*(13), 3299–3308, doi:10.1016/j.gca.2005.02.027.

Koehler, B., E. von Wachenfeldt, D. Kothawala, and L. J. Tranvik (2012), Reactivity continuum of dissolved organic carbon decomposition in lake water, *J. Geophys. Res.*, *117*, G01024, doi:10.1029/2011JG001793.

Mann, P. J., A. Davydova, N. Zimov, R. G. M. Spencer, S. Davydov, E. Bulygina, S. Zimov, and R. M. Holmes (2012), Controls on the composition and lability of dissolved organic matter in Siberia's Kolyma River basin, *J. Geophys. Res.*, *117*, G01028, doi:10.1029/2011JG001798.

Marshall, A. G., C. L. Hendrickson, and G. S. Jackson (1998), Fourier transform ion cyclotron resonance mass spectrometry: A primer, *Mass Spectrom. Rev.*, *17*(1), 1–35, doi:10.1002/(SICI)1098-2787(1998)17:1<1::AID-MAS1>3.0.CO;2-K.

Mayer, L. M., R. G. Keil, S. A. Macko, S. B. Joye, K. C. Ruttenberg, and R. C. Aller (1998), Importance of suspended participates in riverine delivery of bioavailable nitrogen to coastal zones, *Global Biogeochem. Cycles*, *12*(4), 573–579, doi:10.1029/98GB02267.

McKnight, D. M., E. W. Boyer, P. K. Westerhoff, P. T. Doran, T. Kulbe, and D. T. Andersen (2001), Spectrofluorometric characterization of dissolved organic matter for indication of precursor organic material and aromaticity, *Limnol. Oceanogr.*, *46*(1), 38–48, doi:10.4319/lo.2001.46.1.0038.

McLaughlin, C., and L. A. Kaplan (2013), Biological lability of dissolved organic carbon in stream water and contributing terrestrial sources, *Freshwater Sci.*, *32*(4), 1219–1230, doi:10.1899/12-202.1.

Michaelson, G. J., C. L. Ping, G. W. Kling, and J. E. Hobbie (1998), The character and bioactivity of dissolved organic matter at thaw and in the spring runoff waters of the arctic tundra North Slope, Alaska, *J. Geophys. Res.*, *103*, 28,939–28,946, doi:10.1029/98JD02650.

Murphy, K. R., C. A. Stedmon, T. D. Waite, and G. M. Ruiz (2008), Distinguishing between terrestrial and autochthonous organic matter sources in marine environments using fluorescence spectroscopy, *Mar. Chem.*, *108*(1–2), 40–58, doi:10.1016/j.marchem.2007.10.003.

Newbold, J. D., T. L. Bott, L. A. Kaplan, B. W. Sweeney, and R. L. Vannote (1997), Organic matter dynamics in White Clay Creek, Pennsylvania, USA, *J. N. Am. Benthol. Soc.*, *16*(1), 46–50, stable URL: http://www.jstor.org/stable/1468231.

Ohno, T., Z. He, R. L. Sleighter, C. W. Honeycutt, and P. G. Hatcher (2010), Ultrahigh resolution mass spectrometry and indicator species analysis to identify marker components of soil- and plant biomass-derived organic matter fractions, *Environ. Sci. Technol.*, *44*(22), 8594–8600, doi:10.1021/es101089t.

Reemtsma, T. (2009), Determination of molecular formulas of natural organic matter molecules by (ultra-) high-resolution mass spectrometry: Status and needs, *J. Chromatogr. A*, *1216*(18), 3687–3701, doi:10.1016/j.chroma.2009.02.033.

Richey, J. E., J. M. Melack, A. K. Aufdenkampe, V. M. Ballester, and L. L. Hess (2002), Outgassing from Amazonian rivers and wetlands as a large tropical source of atmospheric CO_2, *Nature*, *416*(6881), 617–620, doi:10.1038/416617a.

Sabine, C. L., et al. (2004), The oceanic sink for anthropogenic CO_2, *Science*, *305*(5682), 367–371, doi:10.1126/science.1097403.

Sleighter, R. L., and P. G. Hatcher (2007), The application of electrospray ionization coupled to ultrahigh resolution mass spectrometry for the molecular characterization of natural organic matter, *J. Mass Spectrom.*, *42*(5), 559–574, doi:10.1002/jms.1221.

Sleighter, R. L., and P. G. Hatcher (2008), Molecular characterization of dissolved organic matter (DOM) along a river to ocean transect of the lower Chesapeake Bay by ultrahigh resolution electrospray ionization Fourier transform ion cyclotron resonance mass spectrometry, *Mar. Chem.*, *110*(3–4), 140–152, doi:10.1016/j.marchem.2008.04.008.

Sleighter, R. L., and P. G. Hatcher (2011), Fourier transform mass spectrometry for the molecular level characterization of natural organic matter: Instrument capabilities, applications, and limitations, in *Fourier Transforms—Approach to Scientific Principles*, edited by G. Nikolic, pp. 295–320, InTech, Vienna, stable URL: http://www.intechopen.com/articles/show/title/fourier-transform-mass-spectrometry-for-the-molecular-level-characterization-of-natural-organic-matt.

Sleighter, R. L., G. A. McKee, Z. Liu, and P. G. Hatcher (2008), Naturally present fatty acids as internal calibrants for Fourier transform mass spectra of dissolved organic matter, *Limnol. Oceanogr.: Methods*, *6*, 246–253, doi:10.4319/lom.2008.6.246.

Sleighter, R. L., G. A. McKee, and P. G. Hatcher (2009), Direct Fourier transform mass spectral analysis of natural waters with low dissolved organic matter, *Org. Geochem.*, *40*(1), 119–125, doi:10.1016/j.orggeochem.2008.09.012.

Sleighter, R. L., Z. Liu, J. Xue, and P. G. Hatcher (2010), Multivariate statistical approaches for the characterization of dissolved organic matter analyzed by ultrahigh resolution mass spectrometry, *Environ. Sci. Technol.*, *44*(19), 7576–7582, doi:10.1021/es1002204.

Sleighter, R. L., H. Chen, A. S. Wozniak, A. S. Willoughby, P. Caricasole, and P. G. Hatcher (2012), Establishing a measure of reproducibility of ultrahigh-resolution mass spectra for complex mixtures of natural organic matter, *Anal. Chem.*, *84*(21), 9184–9191, doi:10.1021/ac3018026.

Stedmon, C. A., and S. Markager (2005), Tracing the production and degradation of autochthonous fractions of dissolved organic matter by fluorescence analysis, *Limnol. Oceanogr.*, *50*(5), 1415–1426, doi:10.4319/lo.2005.50.5.1415.

Stenson, A. C., W. M. Landing, A. G. Marshall, and W. T. Cooper (2002), Ionization and fragmentation of humic substances in electrospray ionization Fourier transform-ion cyclotron resonance mass spectrometry, *Anal. Chem.*, *74*(17), 4397–4409, doi:10.1021/ac020019f.

Stenson, A. C., A. G. Marshall, and W. T. Cooper (2003), Exact masses and chemical formulas of individual Suwannee River fulvic acids from ultrahigh resolution electrospray ionization Fourier transform ion cyclotron resonance mass spectra, *Anal. Chem.*, *75*(6), 1275–1284, doi:10.1021/ac026106p.

Stubbins, A., R. G. M. Spencer, H. Chen, P. G. Hatcher, K. Mopper, P. J. Hernes, V. L. Mwamba, A. M. Mangangu, J. N. Wabakanghanzi, and J. Six (2010), Illuminated darkness: Molecular signatures of Congo River dissolved organic matter and its photochemical alteration as revealed by ultrahigh precision mass spectrometry, *Limnol. Oceanogr.*, *55*(4), 1467–1477, doi:10.4319/lo.2010.55.3.1467.

Stubbins, A., et al. (2012), Anthropogenic aerosols as a source of ancient dissolved organic matter in glaciers, *Nat. Geosci.*, *5*(3), 198–201, doi:10.1038/ngeo1403.

Stubbins, A., P. A. del Giorgio, M. Berggren, J. F. Lapierre, and T. Dittmar (2013), What's in an EEM? Molecular signatures associated with dissolved organic fluorophores, paper presented at the Association for the Sciences of Limnology and Oceanography (ASLO) 2013 Aquatic Sciences Meeting, New Orleans, La.

Sweeney, B. W. (1993), Effects of streamside vegetation on macroinvertebrate communities of White Clay Creek, *Proc. Acad. Nat. Sci. Philadelphia*, *144*, 291–340, stable URL: http://www.jstor.org/stable/4065013.

Tranvik, L. J., and S. Bertilsson (2001), Contrasting effects of solar UV radiation on dissolved organic sources for bacterial growth, *Ecol. Lett.*, *4*(5), 458–463, doi:10.1046/j.1461-0248.2001.00245.x.

Tranvik, L. J., et al. (2009), Lakes and reservoirs as regulators of carbon cycling and climate, *Limnol. Oceanogr.*, *54*(6), 2298–2314, doi:10.4319/lo.2009.54.6_part_2.2298.

Vähätalo, A. V., H. Aarnos, and S. Mäntyniemi (2010), Biodegradability continuum and biodegradation kinetics of natural organic matter described by the beta distribution, *Biogeochemistry*, *100*(1–3), 227–240, doi:10.1007/s10533-010-9419-4.

Volk, C. J., C. B. Volk, and L. A. Kaplan (1997), Chemical composition of biodegradable dissolved organic matter in streamwater, *Limnol. Oceanogr.*, *42*(1), 39–44, stable URL: http://www.jstor.org/stable/2838860.

Ward, N. D., R. G. Keil, P. M. Medeiros, D. C. Brito, A. C. Cunha, T. Dittmar, P. L. Yager, A. V. Krusche, and J. E. Richey (2013), Degradation of terrestrially derived macromolecules in the Amazon River, *Nat. Geosci.*, *6*(7), 530–533, doi:10.1038/ngeo1817.

Westrich, J. T., and R. A. Berner (1984), The role of sedimentary organic matter in bacterial sulfate reduction: The G model tested, *Limnol. Oceanogr.*, *29*(2), 236–249.

Wetzel, R. G. (2003), Dissolved organic carbon: Detrital energetics, metabolic regulators, and drivers of ecosystem stability of aquatic ecosystems, in *Aquatic Ecosystems- Interactivity of Dissolved Organic Matter*, edited by S. E. G. Findlay and R. L. Sinsabaugh, pp. 455–477, Academic Press, San Diego.

Wickland, K. P., J. C. Neff, and G. R. Aiken (2007), Dissolved organic carbon in Alaskan boreal forest: Sources, chemical characteristics, and biodegradability, *Ecosystems*, *10*(8), 1323–1340, doi:10.1007/s10021-007-9101-4.

Yamashita, Y., and E. Tanoue (2003), Chemical characterization of protein-like fluorophores in DOM in relation to aromatic amino acids, *Mar. Chem.*, *82*(3–4), 255–271, doi:10.1016/S0304-4203(03)00073-2.